HAL open science

Synthesis of TiO2(110) ultra-thin films on W(100) and their reactions with H2O

J. Matharu, Gregory Cabailh, G. Thornton

To cite this version:

J. Matharu, Gregory Cabailh, G. Thornton. Synthesis of TiO2(110) ultra-thin films on W(100) and their reactions with H2O. Surface Science : A Journal Devoted to the Physics and Chemistry of Interfaces, 2013, 616, pp.198-205. 10.1016/j.susc.2013.05.020 . hal-01229163

HAL Id: hal-01229163

https://hal.science/hal-01229163v1

Submitted on 14 Dec 2015

HAL is a multi-disciplinary open access archive for the deposit and dissemination of scientific research documents, whether they are published or not. The documents may come from teaching and research institutions in France or abroad, or from public or private research centers.

L'archive ouverte pluridisciplinaire **HAL**, est destinée au dépôt et à la diffusion de documents scientifiques de niveau recherche, publiés ou non, émanant des établissements d'enseignement et de recherche français ou étrangers, des laboratoires publics ou privés.

Distributed under a Creative Commons Attribution 4.0 International License

Surface Science 616 (2013) 198–205

Contents lists available at SciVerse ScienceDirect

Surface Science

journal homepage: www.elsevier.com/locate/susc

Synthesis of TiO_2(110) ultra-thin films on W(100) and their reactions with H_2O

J. Matharu [a], G. Cabailh [a,b], G. Thornton [a,*]

[a] London Centre for Nanotechnology and Chemistry Department, University College London, 20 Gordon Street, London WC1H 0AJ, UK
[b] Institut des Nanosciences de Paris, Université Paris 6 — UPMC and CNRS, 4 Place Jussieu, 75005 Paris, France

ARTICLE INFO

Article history:
Received 29 May 2013
Accepted 31 May 2013
Available online 14 June 2013

Keywords:
TiO_2
Thin films
XPS
LEED
H_2O

ABSTRACT

We present a study of the growth and reactivity of ultra-thin films of TiO_2 grown on W(100). Three approaches to film growth are investigated, each resulting in films that show order in low-energy diffraction (LEED) and a low level of non-stoichiometry in X-ray photoelectron spectroscopy (XPS). H_2O is used as a probe of the reactivity of the films, with changes in the Ti 2*p* and O 1*s* core levels being monitored by XPS. Evidence for the dissociation of H_2O on the TiO_2(110) ultra-thin film surface is adduced. These results are discussed with reference to related studies on native TiO_2(110).

© 2013 Elsevier B.V. Open access under CC BY license.

1. Introduction

Thin films can mimic the surfaces of their bulk counterparts [1] and provide a means to modify stoichiometry in a more controlled fashion. Epitaxial ultra-thin films can be grown on metallic substrates that are well-ordered and exhibit sufficient conducting character to enable study by electron spectroscopy and STM [2–6]. Both of these factors provide a motivation for the current work on TiO_2 ultra-thin films. Bennett et al. have previously grown thin films of TiO_2 using two deposition methods [7]: Ti deposition on a clean W(100) followed by post-oxidation and Ti deposition on a pre-oxidised W(100) surface. The latter method relies on the formation of a p(2 × 1)-O adlayer following exposure of W(100) to O_2 [8,9]. This results in a unit cell of dimensions 6.32 × 3.16 Å^2, which is comparable to the TiO_2 (110) unit cell, 6.49 × 2.96 Å^2. The mismatch between these two cells is 2.7% × −6%. In the earlier work, Bennett et al. show that their TiO_2 thin films have the rutile structure when using both preparation methods.

Previous structural characterisation work on ultra-thin (<1 nm thickness) films of rutile TiO_2(110) is restricted to the use of Ni(110) [10,11], $Ni_{94}Ti_6$ (110) [12], Mo(100), (110) and (112) [13–15] and more recently Ag(100) [16] as substrates. Here we look at the extension of the earlier work on thin films on W(100) [7] to the ultra-thin regime, using the reaction with water to provide additional characterisation to LEED and XPS. This complements previous work on ultrathin films on W(100) that examined XPS, UPS and infra-red spectra [17].

Defects in the form of O-vacancies on TiO_2(110) are known to be important in the reaction with H_2O [18,19]. Hence, one means of investigating the defect character of TiO_2(110) ultrathin films is to use H_2O as a probe molecule [20]. Surface science studies of the H_2O interaction with TiO_2(110) surface have built up a picture of the adsorption process and revealed evidence for the presence of surface hydroxyls (as a result of dissociation) at room temperature, accompanied by an increase in Ti^{3+} states [21]. Experiments from Walle et al. suggest that both molecular and dissociative adsorption of H_2O occur when a monolayer of water is deposited on a nominally defect free rutile TiO_2(110) at 210 K [22]. Only dissociative adsorption of water is observed at room temperature, which involves dissociation at O-vacancies [22,23]. Recent first-principle simulations suggest that water does not dissociate on the defect free surface [24].

Scanning tunnelling microscopy (STM) and non-contact atomic force microscopy (NC-AFM) have provided insight into the mechanism of dissociation [23,25–28]. The currently accepted mechanism is that H_2O molecules adsorb at O vacancy sites (O_{vac}) and dissociate, resulting in a pair of hydroxyls in the bridging row (OH_b): one in place of the original O_{vac}, and a second formed from the dissociated H atom and another bridging row oxygen atom (O_b). The resulting OH_b pair and its related charges play an important role in reactivity of the surface with O_2 [28]. Here we examine the morphology of TiO_2(110) ultra-thin films, their electronic structure as well as their reactivity with H_2O.

2. Experimental

Experiments were conducted in an ultra high vacuum (UHV) chamber with a base pressure of 3 × 10^{-10} mbar. Data were recorded at room

* Corresponding author. Tel.: +44 2076797979.
E-mail addresses: matharujai@gmail.com (J. Matharu), cabailh@insp.upmc.fr (G. Cabailh), g.thornton@ucl.ac.uk (G. Thornton).

0039-6028 © 2013 Elsevier B.V. Open access under CC BY license.
http://dx.doi.org/10.1016/j.susc.2013.05.020

temperature, using an unpolarised Mg Kα radiation source ($h\nu = 1253.6$ eV) and a *VSW/Omicron* EA125 hemispherical analyser. The angle of incidence of X-ray photons was 67.5° with respect to the surface normal, with photoelectrons collected at normal emission. A pass-energy of 40 eV was used, giving an energy resolution (full width at half maximum) of 0.3 eV. Binding energies are measured relative to the Fermi level, which was recorded from the Ta sample holder.

The W(100) crystal (Surface Preparation Laboratory) was cleaned by Ar^+ sputtering, followed by repeated cycles of annealing in 1×10^{-7} mbar of high purity O_2 (SIP Analytical, 99.5%) at 1100 K and flash annealing in UHV to 2000 K to remove the principal contaminants (O and C) [29]. The clean surface was characterised by a sharp (1 × 1) LEED pattern and the absence of O 1*s* and C 1*s* peaks in XPS spectra.

Ti was deposited using a home-built electron beam evaporator. The doser was calibrated using the intensity ratios of the Ti 2*p*, W 4*p* and W 4*d* XPS peaks. Breakpoints in the ratios indicate monolayer coverage [30] and can be used to monitor the amount of Ti deposited. Oxidation of deposited Ti was achieved by annealing in 1×10^{-7} mbar O_2 at 800 K for 2 h. Films were characterised by a TiO_2(110) (1 × 1) LEED pattern with additional spots along the principal azimuths [7]. Film thicknesses were estimated from the areas of the Ti 2*p* and W 4*d* XPS peaks using the method described by Susaki et al. [31], correcting the peak areas to account for ionisation cross sections and for the analyser transmission function. One monolayer equivalent (MLE) is defined as the number of TiO_2 surface unit cells that will uniformly cover the surface of the W(100) substrate. De-ionised H_2O was degassed using freeze-pump-thaw cycles. The sample was exposed to H_2O as well as O_2 by backfilling the chamber to a pressure of 1×10^{-7} mbar.

3. Results

3.1. TiO_2 thin film growth

Three approaches to ultra-thin film growth were used, the first two being similar to those employed by McCavish et al. who have studied a coverage regime from 5 to 30 monolayers [7]. In one approach, Ti was deposited in UHV onto a clean W(100) surface (two-stage growth). The second method consisted of depositing Ti in UHV onto a pre-oxidised W(100) surface (pre-oxidised growth) and the third depositing Ti in a partial pressure of O_2 (reactive growth). All these depositions were followed by post-oxidation in O_2. Ti deposited on the clean W surface is metallic in nature. This is evident from XPS of the Ti 2*p* region, showing asymmetric Doniach–Sunjic type peaks [32] at $E_B = 454.7$ eV ($2p_{3/2}$) and 460.7 eV ($2p_{1/2}$) (1.6 MLE film, Fig. 1(a)) [33]. After annealing in 1×10^{-7} mbar O_2 at 800 K for 2 h, oxidation causes the Ti 2*p* core levels to shift to 459.0 eV ($2p_{3/2}$) and 464.7 eV ($2p_{1/2}$), typical of Ti^{4+} [34,35] (Fig. 1(a)).

In the case of pre-oxidised growth, where Ti is deposited on the W surface previously annealed in 1×10^{-7} mbar O_2 at 800 K for 3 min, the Ti 2*p* XPS peaks are broader than for Ti deposited on the clean W surface (1.2 MLE film, Fig. 1(b)). This broadening can be assigned to the presence of oxidised species of Ti (i.e. Ti^{2+} and Ti^{3+}). The main peaks of these species are positioned at $E_B = 457.1$ eV (Ti^{3+}) and 455.4 eV (Ti^{2+}). As for the case of the two-stage growth, these peaks shift to positions associated with Ti^{4+} states after a 2 h anneal in O_2.

Depositing Ti in a background pressure of 1×10^{-7} mbar O_2 initially results in a Ti 2*p* XPS spectrum showing contributions from Ti^{4+} states as well as reduced Ti^{3+} and Ti^{2+} states, indicating incomplete oxidation [34] as shown for a 1.2 MLE film (Fig. 1(c)). After a 2 h anneal in O_2, the Ti 2*p* core level width decreases as Ti^{2+} states (at $E_B = 455.4$ eV and 460.8 eV) are completely removed. By contrast the Ti^{3+} states are not completely removed, indicating that the film is slightly substoichiometric.

TiO_2(110) films between 0.2 and 5.7 MLE thick were synthesised. In all cases, on deposition of Ti the observed LEED pattern has a very high background with faint (1 × 1) spots from the W(100) substrate. This indicates the absence of long range order associated with the deposited Ti using the three different growth methods. Following annealing in O_2, oxidised films produce LEED patterns (Fig. 2(c)) that are a composite of the (1 × 1) spots from the W(100) substrate (Fig. 2(a)) and the (1 × 1) spots from an ordered TiO_2(110) surface (Fig. 2(b)). For films of thickness <1 MLE, the LEED beams are faint, likely due to incomplete coverage of the W(100) substrate and oxidation of regions of bare W. For films as thick as 5.7 MLE, the substrate diffraction spots are still visible, indicating that the thin films do not entirely cover the substrate surface.

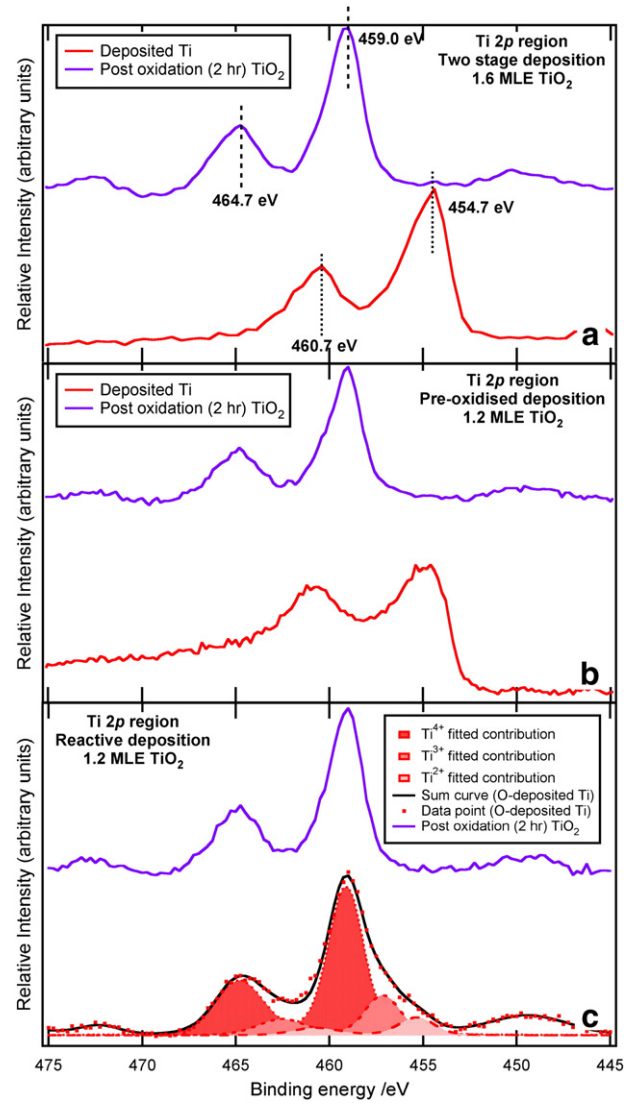

Fig. 1. MgKα XPS spectra ($h\nu = 1253.6$ eV) of W(100) showing (a) the shift in E_B of the Ti 2*p* core levels after oxidation in 1×10^{-7} mbar O_2 for 2 h at 800 K for the two stage growth, (b) the broadened Ti 2*p* core levels of Ti deposited on an oxidised W(100) surface (bottom) and the shift to fully oxidised peaks after oxidation in 1×10^{-7} mbar O_2 for 2 h at 800 K (top) and (c) the mixed valence Ti states on depositing Ti in 1×10^{-7} mbar O_2 (bottom), and the removal of these states on oxidation in 1×10^{-7} mbar O_2 for 2 h at 800 K (top, blue). Spectra are normalised to the same maximum intensity and Shirley backgrounds have been subtracted. The peak at 449 eV corresponds to the Ti 2*p* satellites from Mg $K\alpha_{3,4}$ excitation. Ti 2*p* spectra were fitted with three doublets (Voigt functions) corresponding to the Ti^{2+} (light red), Ti^{3+} (red) and Ti^{4+} (dark red) contributions, as shown for the reactive deposition method (c). The sum of the fitted contributions is represented by the black line and the experimental data by red dots. A polynomial plus Shirley background was subtracted. The peak widths, branching ratio, and spin-orbit-splitting were kept constant throughout and are summarised in Table 1.

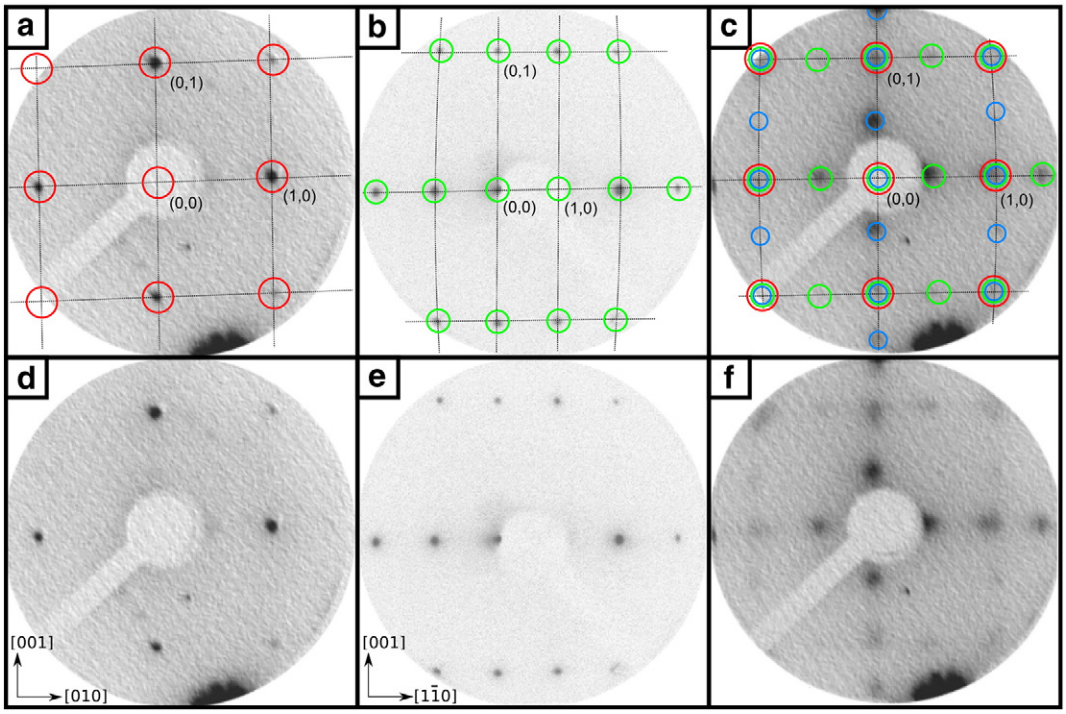

Fig. 2. LEED patterns for (a) the clean W(100) surface (beam energy, $E_{beam} = 55$ eV), with red circles indicating (1 × 1) spots; (b) a reference TiO_2(110) crystal ($E_{beam} = 66$ eV), with the green circles indicating TiO_2(110) (1 × 1) spots and (c) a 5.8 MLE TiO_2 film grown by the pre-oxidised method on W(100) ($E_{beam} = 55$ eV). The green and blue circles indicate the two TiO_2 domains. The figures are reproduced (d–f) without the symbols for clarity. The azimuthal orientations of the single crystals are indicated.

The final pattern is a two-domain (2 × 1) with respect to the initial W(100) pattern, with two TiO_2 domains rotated 90° and aligned with the main directions of the substrate, as observed in the earlier work [7].

Examination of Ti 2*p* XPS spectra shows that films synthesised using the pre-oxidised method are not completely stoichiometric and that contributions from both Ti^{3+} and Ti^{4+} states are present (Fig. 3). Using the fitting parameters in Table 1, we use the Ti 2*p* spectrum to estimate the % Ti^{3+} states (Table 2). Non-stoichiometry may arise due to strain in the films resulting from the lattice mismatch and from surface defects. A correlation between thickness and non-stoichiometry has been previously observed [7] with non-stoichiometry decreasing with increased thickness. Curve fitting of the corresponding O 1*s* XPS spectra reveals two contributions (Fig. 3), one centred around a binding energy of 530.4 eV that corresponds to oxygen in the selvedge, and a satellite peak, denoted S_1 shifted + 1.4 eV from the main peak (fitting parameters shown in Table 1). S_1 was assigned to two-fold bridging oxygen atoms (O_b) on the TiO_2 surface in earlier work [36–38]. However, more recent studies have instead suggested that this peak is due to OH_b arising from reaction with residual water in the background vacuum [11,39]. The S_1 contribution, expressed as a percentage of the total O 1*s* peak area, is greater in films <1 MLE TiO_2 thick.

The nature of the substrate–film interface can be investigated by comparison of the W 4*d* XPS spectra for different stages of the growth process [7]. Upon adsorption of oxygen there is a slight broadening of the W 4*d* XPS peaks at higher binding energy compared with the clean surface (Fig. 4(a)). Streaking along the principal azimuths is also observed in the LEED pattern and with sufficient exposure to oxygen this sharpens to a (4 × 1) pattern as observed in [40]. There is no apparent change between the W 4*d* XPS spectra of the clean W surface and a Ti-deposited W surface (Fig. 4(b)). This is also the case between the W 4*d* spectrum of a fully oxidised TiO_2 film and the oxidised W surface (Fig. 4(c)).

3.2. Interaction with H_2O

As a preliminary measurement, a clean W(100) surface was exposed to up to 100 l H_2O (1 L = 1.32×10^{-6} mbar s^{-1}). There has been a previous study of H_2O adsorption on W(100), which employed synchrotron radiation photoemission [41]. This indicated dissociative adsorption with formation of W–O bonds. Fig. 5(a) shows the changes in O 1*s* XPS spectra as H_2O exposure increases. Even with very thorough cleaning, a trace amount of oxygen is present on the nominally clean surface. The intensity of this peak increases on exposure to H_2O and it can be fitted with two Gaussian–Lorentzian singlet peaks at 530.5 eV and 532.9 eV. Using the area of these peaks and the area of the W 4*d* XPS spectra, the atomic concentration ratio of O and W is seen to increase exponentially (Fig. 5(b)) to a saturation limit of 0.15 and 0.05 for the peaks at 530.5 eV and 532.9 eV, respectively. The peak at 530.5 eV corresponds to what is expected for adsorbed atomic oxygen [42]. An E_B of 532.9 eV corresponds to that expected for molecular water [41].

TiO_2 thin films prepared by the pre-oxidised W(100) method were exposed to ≤200 L H_2O in stages at 293 K. No change was observed in the LEED pattern, aside from attenuation of spots indicating adsorption without long range order. Changes to the stoichiometry of films upon H_2O exposure were monitored through the evolution of the Ti 2*p* XPS spectra. These are shown for two of the films, with thicknesses of 0.9 MLE TiO_2 (Fig. 6(a–c)) and 5.3 MLE TiO_2 (Fig. 7(a–c)). In both cases, there is an increase in the Ti^{3+} concentration.

For the thinnest film, increases on the lower E_B side of the Ti 2*p* doublet are apparent upon water exposure (see Fig. 6(a)). The difference spectrum for each exposure shows a doublet at 458.1 eV and 463.5 eV up to 187 L H_2O exposure, which evidences the presence of Ti^{3+} states (Fig. 6(b)). For large exposure, the doublet peak in the difference spectra gains some asymmetry to lower E_B. This can be fitted with another

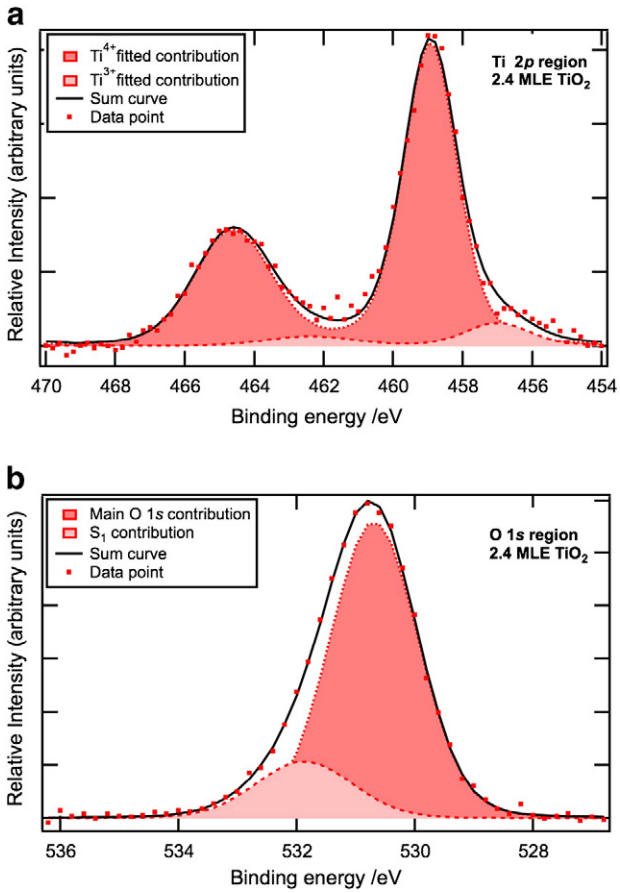

Fig. 3. MgKα XPS spectra ($h\upsilon = 1253.6$ eV) after Shirley background subtraction of a 2.4 MLE thick TiO_2 film grown using the pre-oxidised W(100) method. (a) Ti 2*p* region showing contributions from Ti^{3+} and Ti^{4+} ions, as estimated by fitting with two Gaussian–Lorentzian doublets. Ti^{3+} ions make up 9% of the overall Ti contribution. (b) O 1*s* region showing contributions from the main O 1*s* XPS peak and the S_1 satellite. The latter accounts for 27% of the total O 1*s* XPS peak area.

doublet at 455.4 eV and 460.8 eV and suggests the presence of Ti^{2+} states [34]. By peak fitting and comparing peak areas, the relative concentration of Ti^{3+} and Ti^{2+} can be estimated (Fig. 8). Plotting these values against exposure (Fig. 6(c)) shows an increase in $\%Ti^{3+}$, nearing a maximum at 37% Ti^{3+} after 100 L exposure. A shallower increase to a maximum of 20% Ti^{2+} is observed, with Ti^{2+} features not present below 7 L exposure. In thicker films, no Ti^{2+} features are observed. However, an increase in Ti^{3+} concentration is still observed in the Ti 2*p* spectra (Fig. 7(a)). The doublet peak appearing in difference spectra is more symmetric and can be fitted with a single doublet with XPS peaks at 458.1 eV and 463.5 eV, corresponding to Ti^{3+} features (Fig. 7(b)). The increase in $\%Ti^{3+}$ features reaches a maximum of 18% at 60 L for the 5.3 MLE film.

Table 1
Parameters used in Ti 2*p* (Figs. 1, 3 and 8) and O 1*s* (Fig. 3) fitting procedures, showing peak position and Gaussian–Lorentzian (Voigt function) full-width at half-maximum (FWHM) values.

		Position/eV	FWHM/eV
Ti^{4+}	$2p_{3/2}$	459.0	2.16
	$2p_{1/2}$	464.8	2.97
Ti^{3+}	$2p_{3/2}$	457.1	2.20
	$2p_{1/2}$	462.5	2.99
Ti^{2+}	$2p_{3/2}$	455.4	2.22
	$2p_{1/2}$	460.8	3.02
O 1*s*		530.4	1.82
S_1		531.8	2.06

Table 2
Summary of initial values for $\%Ti^{3+}$ and $\%S_1$ for TiO_2(110) ultra-thin films on W(100) of varying thickness prepared by the pre-oxidised method. The corresponding figures are given for the spectra following a saturation exposure to water at 1×10^{-8} mbar.

TiO_2 thickness /MLE	Initial $\%Ti^{3+}$	Initial $\%S_1$	Saturation $\%Ti^{3+}$	Saturation $\%S_1$
0.9	5.0 ± 2.4	26.3 ± 1.2	37.2 ± 3.1	35.0 ± 1.8
1.6	6.6 ± 2.1	27.0 ± 1.3	15.3 ± 1.2	29.4 ± 1.0
4.2	4.5 ± 2.4	29.7 ± 1.4	15.3 ± 1.1	32.6 ± 1.1
5.3	0.0 ± 1.0	24.0 ± 2.7	17.5 ± 2.8	31.1 ± 1.4

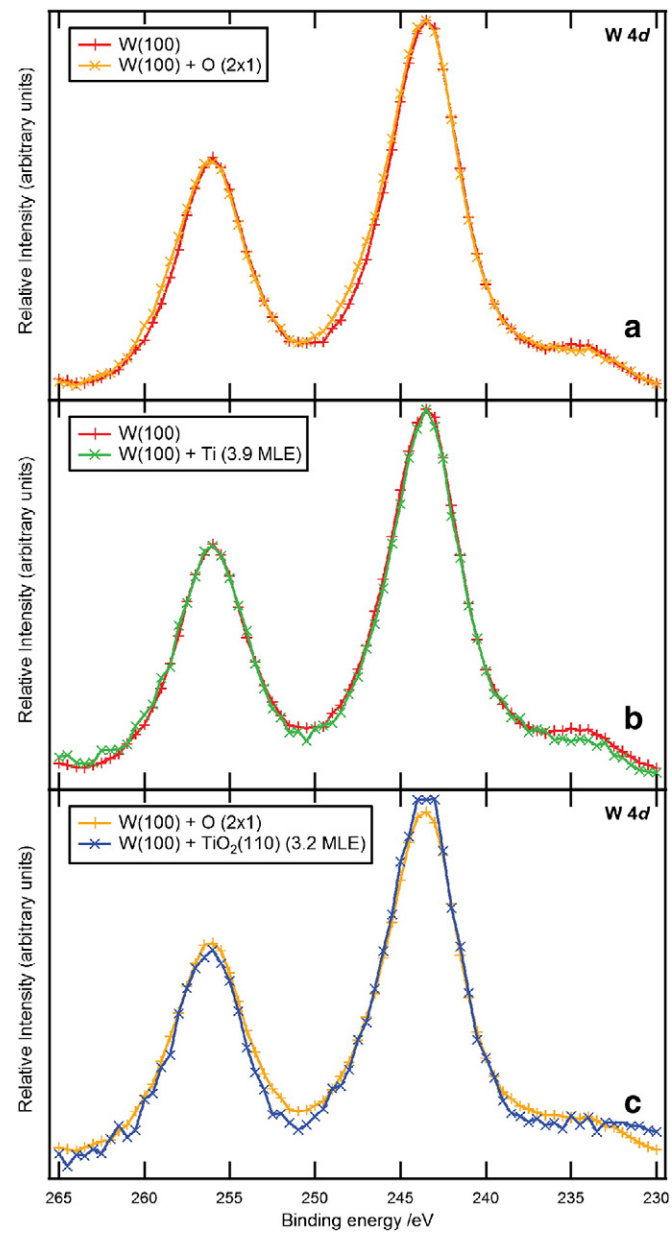

Fig. 4. Comparison of the MgKα W 4*d* XPS spectra ($h\upsilon = 1253.6$ eV) for (a) W(100) and W(100)-(2 × 1)-O surfaces, (b) W(100) and Ti-deposited (3.9 MLE Ti) W(100) surfaces, and (c) W(100)-(2 × 1)-O surface and a fully oxidised TiO_2(110) thin film on W(100) (grown using the two-stage method). Shirley backgrounds have been subtracted and spectra are normalised to the same maximum intensity.

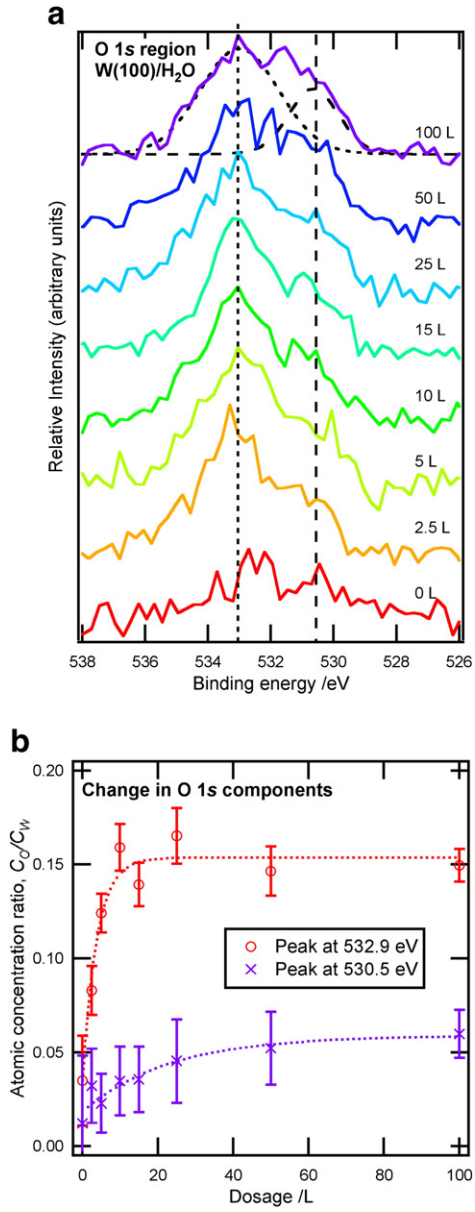

Fig. 5. (a) MgKα XPS spectra ($h\nu = 1253.6$ eV) of the O 1*s* region for W(100) exposed to H_2O at 300 K. Shirley backgrounds have been subtracted. (b) Atomic concentration ratio C_O/C_W as a function of exposure to H_2O, where C_O and C_W correspond to the peak areas of O 1*s* and W 4*d*, respectively. The ratio in atomic concentration increases exponentially to a saturation limit of 0.15 and 0.05 for the peaks at 532.9 eV (red) and 530.5 eV (blue), respectively.

Changes in the O 1*s* XPS spectra are shown for the same two films: 0.9 MLE TiO_2 (Fig. 6(d–f)) and 5.3 MLE (Fig. 7(d–f)). An increase at higher E_B is observed upon increasing H_2O exposure (Figs. 6(d), 7(d)). This increase is more apparent in the difference spectra of each scan after subtraction of the 0 L H_2O exposure spectrum (Figs. 6(e), 7(e)). Peak fitting of the difference spectra reveal an increase in a feature at an E_B of 531.8 eV, corresponding to the position of the S_1 satellite referred to above. This increases to a maximum value of 35% of the total O 1*s* area for the 0.9 MLE film and 31% for the 5.3 MLE film. The higher increase for the thinner film can be related to the higher increase in Ti^{3+} states which are twice as large for the 0.9 MLE film (~32%) compared to the thicker films (~16%). For the 0.9 MLE film, an increase is also seen in a feature at an E_B of 533.0 eV denoted S_2. Initial and saturation values of $\%Ti^{3+}$ and $\%S_1$ for the films are tabulated in Table 2.

4. Discussion

LEED data indicate that there is no long-range order associated with Ti deposited on W surfaces, but that ordered $TiO_2(110)$ films result post-oxidation. The LEED patterns are sharper for thicker films presumably because the TiO_2 islands are larger and the strain due to the lattice mismatch between the substrate and the film decreases with increasing thickness. The similarity in the Ti 2*p* and O 1*s* XPS spectra for each of the growth methods used suggests that films produced by each route are more or less equivalent. At the temperature at which the films are annealed (800 K), oxygen can diffuse through TiO_2 [43] and films can be completely oxidised regardless of initial conditions. Strain, as well as surface defects such as O_{vac} can also explain the slight non-stoichiometry. The W 4*d* spectrum of the W/TiO_2 interface is similar to the same spectrum for oxidised W, suggesting that the film layer at the substrate interface consists of O atoms rather than Ti.

The increase in Ti^{3+} states on exposure to H_2O suggests dissociation on the TiO_2 thin film surface, with resulting charge transfer from hydroxyl species to Ti^{4+} [21]. The O 1*s* XPS data is consistent with this picture, showing an increase in intensity of the OH peak (S_1), with no increase of a feature at the position expected for molecular H_2O (2.5 to 3.5 eV higher BE). For the 0.9 MLE film the increase in height of S_2 will arise from molecular adsorption on bare areas of W(100)-O. The values of $\%Ti^{3+}$ increase with H_2O exposure for all films (Table 2), whereas Ti^{2+} states are only detected for the exposure of the 0.9 MLE TiO_2 thick film to H_2O. Since the film is of <1 MLE thickness, the W(100)-O surface is not completely covered with TiO_2 and the formation of lower oxides such as TiO is possible, especially at island edges. The asymmetry of the O 1*s* difference spectra upon H_2O exposure for the 0.9 MLE film can also be explained by exposure of the W(100)-O surface to water (Fig. 6e). Changes in the S_1 contribution (531.8 eV) as well as the feature arising from H_2O adsorption on exposed W (532.9 eV), where H_2O oxidises the W surface to WO_3 and WO_{3-x} [42] will contribute intensity to the difference spectra.

In the experiments presented here, the $\%S_1$ increases exponentially to a maximum saturation value and is assigned to the presence of adsorbed hydroxyls. The presence of S_1 prior to H_2O exposure will be due to dissociative adsorption of H_2O from the residual vacuum [11].

5. Conclusions

Three methods of synthesising ultra-thin films of $TiO_2(110)$ on a W(100) substrate have been investigated using XPS and LEED. The resulting films have been found to be equivalent, with films between 0.2 and 5.7 MLE being synthesised. The reactivity of the $TiO_2(110)$ surface has been examined by exposing to H_2O. An increase in adsorbed hydroxyls, OH_b, accompanies an increase in Ti^{3+} states, consistent with an increase in excess charge on the $TiO_2(110)$ surface. Molecular H_2O was not observed spectroscopically except for films of <1 MLE TiO_2 thickness, where regions of exposed WO_x are present and can be hydrated, as shown by exposure of a clean W surface to H_2O. The findings of this study are in line with experiments previously reported in the literature using native surfaces of TiO_2 and on ultra-thin films of $TiO_2(110)$ [10–16]. We note that ultra-thin TiO_2 films grown on W(100) would be suitable for use in electron spin resonance experiments, since the substrate is paramagnetic.

Acknowledgements

This work was supported by the EPSRC (UK) and COST1104. In addition, GT acknowledges the support of a European Research Council Advanced Grant (ENERGYSURF) and a Humboldt Research Award.

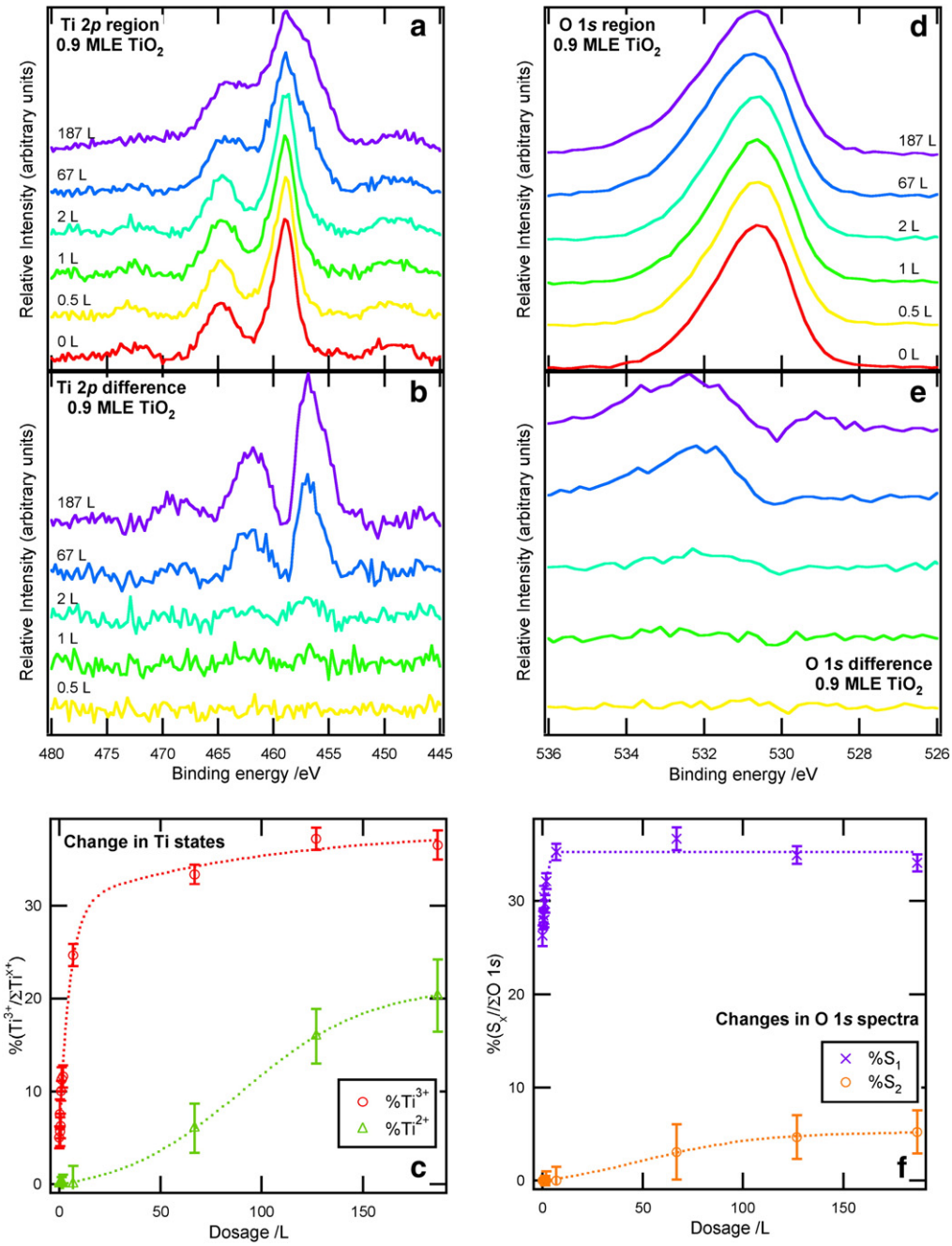

Fig. 6. MgKα XPS spectra ($h\upsilon = 1253.6$ eV) of W(100) after growth of a 0.9 MLE TiO_2 thin film (pre-oxidised growth). The spectra are presented as a function of H_2O exposure up to 187 L at 300 K: (a) Ti 2*p* region spectra at each exposure, (b) difference spectra showing changes compared with the film prior to H_2O exposure, (c) change in $\%Ti^{3+}$ upon H_2O exposure, (d) O 1*s* region spectra as a function of exposure; (e) difference spectra showing changes compared with the film prior to H_2O exposure; (f) change in $\%S_1$ and $\%S_2$ of the O 1*s* signal upon H_2O exposure.

References

[1] S.A. Chambers, Surf. Sci. Rep. 39 (2000) 105.
[2] C.R. Henry, Surf. Sci. Rep. 31 (1998) 231.
[3] R.M. Jaeger, H. Kuhlenbeck, H.-J. Freund, M. Wuttig, W. Hoffmann, R. Franchy, H. Ibach, Surf. Sci. 259 (1991) 235.
[4] G.S. Herman, M.C. Gallagher, S.A. Joyce, C.H.F. Peden, J. Vac. Sci. Technol. B 14 (1996) 1126.
[5] D.C. Grinter, R. Ithnin, C.L. Pang, G. Thornton, J. Phys. Chem. C 114 (2010) 17036.
[6] S.C. Street, C. Xu, D.W. Goodman, Annu. Rev. Phys. Chem. 48 (1997) 43.
[7] N.D. McCavish, R.A. Bennett, Surf. Sci. 546 (2003) 47.
[8] H. Yamazaki, T. Kamisawa, T. Kokubun, T. Haga, S. Kamimizu, K. Sakamoto, Surf. Sci. 477 (2001) 174.
[9] H. Yamazaki, S. Kamimizu, K. Hara, K. Sakamoto, Surf. Sci. 538 (2003) L505.
[10] T.V. Ashworth, G. Thornton, Thin Solid Films 400 (2001) 43.
[11] A.C. Papageorgiou, G. Cabailh, Q. Chen, A. Resta, E. Lundgren, J.N. Andersen, G. Thornton, J. Phys. Chem. C 111 (2007) 7704.
[12] A. Atrei, U. Bardi, G. Rovida, Surf. Sci. 391 (1997) 216.
[13] W.S. Oh, C. Xu, D.Y. Kim, D.W. Goodman, J. Vac. Sci. Technol. A 15 (1997) 1710.
[14] X. Lai, Q. Guo, B.K. Min, D.W. Goodman, Surf. Sci. 487 (2001) 1.
[15] D. Kumar, M.S. Chen, D.W. Goodman, Thin Solid Films 515 (2006) 1475.
[16] A. Atrei, B. Cortigiani, A.M. Ferrari, J. Phys. Condens. Matter 24 (2012) 445005.
[17] R.A. Bennett, J.S. Mulley, M.A. Newton, M. Surman, J. Chem. Phys. 127 (2007) 084707.
[18] M.A. Henderson, Surf. Sci. 355 (1996) 151.
[19] M.A. Henderson, Langmuir 12 (1996) 5093.
[20] C.L. Pang, R. Lindsay, G. Thornton, Chem. Soc. Rev. 37 (2008) 2328.
[21] R.L. Kurtz, R. Stockbauer, T.E. Madey, E. Román, J.L. de Segovia, Surf. Sci. 218 (1989) 178.

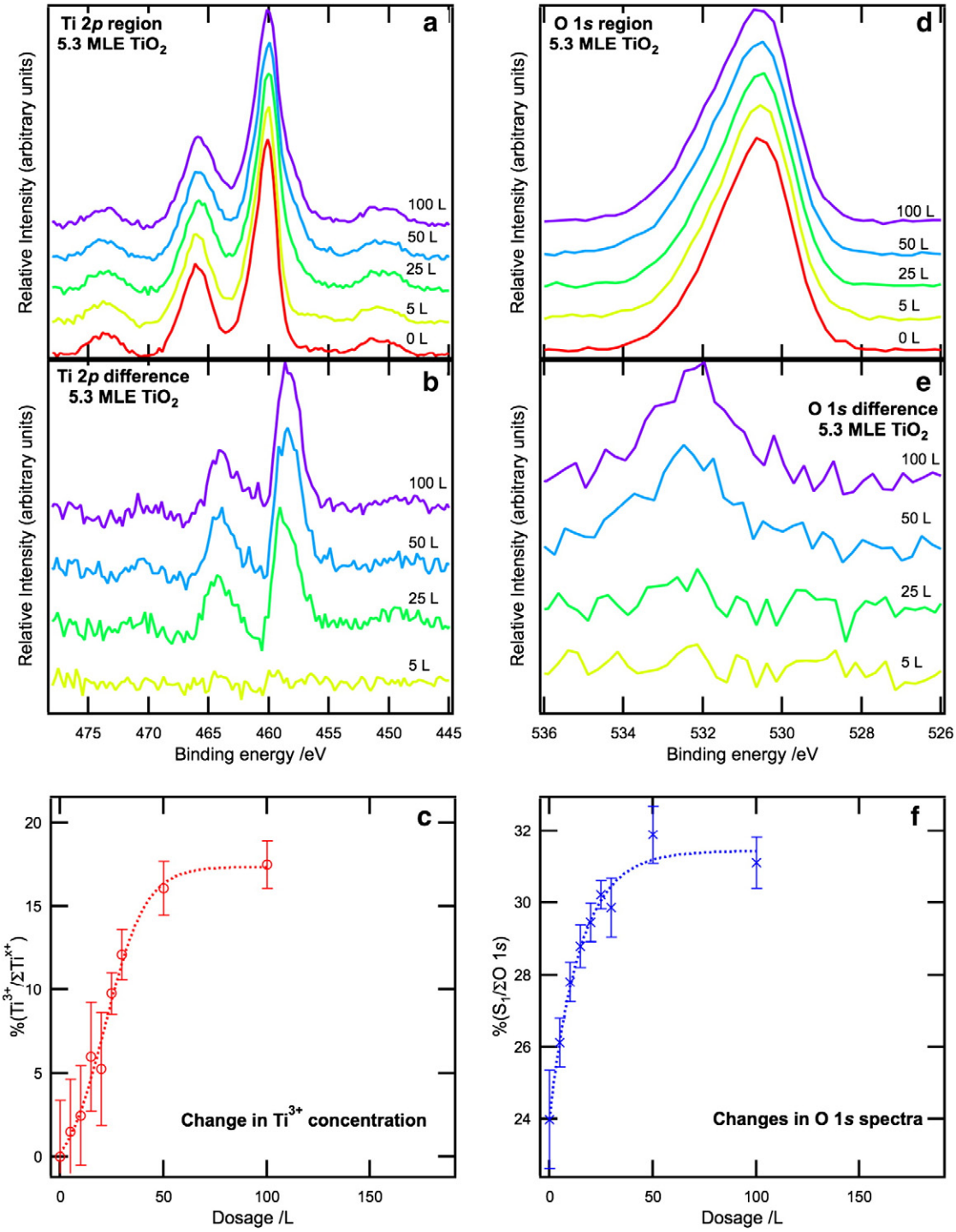

Fig. 7. MgKα XPS spectra ($h\upsilon = 1253.6$ eV) of W(100) after growth of a 5.3 MLE TiO_2(110) thin film (pre-oxidised growth). The spectra are presented as a function of H_2O exposure up to 100 L at 300 K: (a) Ti 2*p* region at each exposure; (b) difference spectra showing changes compared with the film prior to H_2O exposure; (c) change in $\%Ti^{3+}$ upon H_2O exposure; (d) O 1*s* region at each exposure; (e) difference spectra showing changes compared with the film prior to H_2O exposure; (f) change in $\%S_1$ O 1*s* signal upon H_2O exposure. All spectra have had a Shirley background removed.

[22] L.E. Walle, A. Borg, P. Uvdal, A. Sandell, Phys. Rev. B 80 (2009) 235436.
[23] S. Wendt, R. Schaub, J. Matthiesen, E.K. Vestergaard, E. Wahlström, M.D. Rasmussen, P. Thostrup, L.M. Molina, E. Lægsgaard, I. Stensgaard, B. Hammer, F. Besenbacher, Surf. Sci. 598 (2005) 226.
[24] L.-M. Liu, C. Zhang, G. Thornton, A. Michaelides, Phys. Rev. B 82 (2010) 161415R.
[25] I.M. Brookes, C.A. Muryn, G. Thornton, Phys. Rev. Lett. 87 (2001) 266103.
[26] O. Bikondoa, C.L. Pang, R. Ithnin, C.A. Muryn, H. Onishi, G. Thornton, Nat. Mater. 5 (2006) 189.
[27] Z. Zhang, O. Bondarchuk, B.D. Kay, J.M. White, Z. Dohnálek, J. Phys. Chem. B 110 (2006) 21840.
[28] A.C. Papageorgiou, N.S. Beglitis, C.L. Pang, G. Teobaldi, G. Cabailh, Q. Chen, A.J. Fisher, W.A. Hofer, G. Thornton, Proc. Natl. Acad. Sci. 107 (2010) 2391.
[29] M. Grunze, H. Ruppender, O. Elshazly, J. Vac. Sci. Technol. A 6 (1988) 1266.
[30] I. Vaquila, M.C.G. Passeggi Jr., J. Ferrón, Phys. Rev. B 55 (1997) 13925.
[31] T. Susaki, T. Komeda, M. Kawai, Phys. Rev. Lett. 88 (2002) 187602.
[32] S. Doniach, M. Šunjić, J. Phys. C Solid State Phys. 3 (1970) 285.
[33] In: A.C. Thompson, D. Vaughan (Eds.), X-Ray Data Booklet, 2nd edition, Lawrence Berkeley National Laboratory, University of California, 2001, (http://xdb.lbl.gov/xdb.pdf).
[34] B. Siemensmeyer, J.W. Schultze, Surf. Interface Anal. 16 (1990) 309.

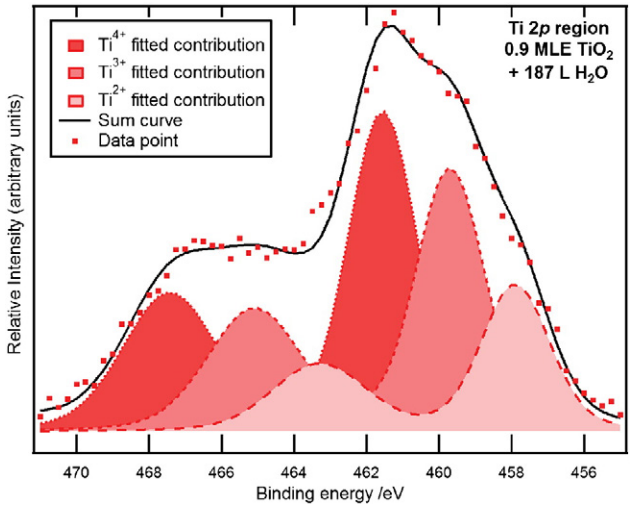

Fig. 8. MgKα XPS spectrum ($h\upsilon = 1253.6$ eV) of a 0.9 MLE TiO_2(110) film (pre-oxidised growth) on W(100) after exposure to 187 L H_2O at 300 K. The spectrum has been Shirley background subtracted. Contributions from Ti^{2+}, Ti^{3+} and Ti^{4+} ions are highlighted. They were estimated by fitting with three Gaussian–Lorentzian doublets. The concentrations of Ti^{2+} and Ti^{3+} are 20% and 37%, respectively.

[35] C.N. Sayers, N.R. Armstrong, Surf. Sci. 77 (1978) 301.
[36] T.K. Sham, M.S. Lazarus, Chem. Phys. Lett. 68 (1979) 426.
[37] E.L. Bullock, L. Patthey, S.G. Steinemann, Surf. Sci. 352–354 (1996) 504.
[38] J. Cardenas, S. Sjöberg, Surf. Sci. 532–535 (2003) 1104.
[39] L.-Q. Wang, D.R. Baer, M.H. Engelhard, A.N. Shultz, Surf. Sci. 344 (1995) 237.
[40] E. Bauer, H. Poppa, Y. Viswanath, Surf. Sci. 58 (1976) 517.
[41] D. Mueller, A. Shih, E. Roman, T. Madey, R. Kutz, R. Stockbauer, J. Vac. Sci. Technol. A 6 (1988) 1067.
[42] In: E. Lassner, W.-D. Schubert (Eds.), Tungsten: Properties, Chemistry, Technology of the Element, Alloys and Chemical Compounds, Springer, New York, 1999.
[43] J.T. Mayer, U. Diebold, T.E. Madey, E. Garfunkel, J. Electron Spectrosc. Relat. Phenom. 73 (1995) 1.